International Journal of Refrigeration 100 (2019) 131–140

Contents lists available at ScienceDirect

International Journal of Refrigeration

journal homepage: www.elsevier.com/locate/ijrefrig

A comprehensive study to evaluate absolute uptake of carbon dioxide adsorption onto composite adsorbent

Bakytnur Berdenova[a], Animesh Pal[b], Mahbubul Muttakin[b,c], Sourav Mitra[d], Kyaw Thu[b,c], Bidyut Baran Saha[b,e,*], Aidarkhan Kaltayev[a,f]

[a] Faculty of Mechanics and Mathematics, Al-Farabi Kazakh National University, 71 al-Farabi Ave., Almaty 050040, Kazakhstan
[b] International Institute for Carbon-Neutral Energy Research (WPI-I2CNER), Kyushu University, 744 Motooka, Nishi-ku, Fukuoka 819-0395, Japan
[c] Interdisciplinary Graduate School of Engineering Sciences, Kyushu University, Kasuga-koen 6-1, Kasuga-shi, Fukuoka 816-8580, Japan
[d] Department of Mechanical Engineering, Indian Institute of Technology, Kharagpur 721302, India
[e] Mechanical Engineering Department, Kyushu University, 744 Motooka, Nishi-ku, Fukuoka 819-0395, Japan
[f] School of Industrial Engineering, Satbayev University, 22a Satpaev str., Almaty 050013, Kazakhstan

ARTICLE INFO

Article history:
Received 8 September 2018
Revised 21 December 2018
Accepted 7 January 2019
Available online 9 January 2019

Keywords:
Adsorption
Absolute uptake
Composite
Isotherm model
Thermal conductivity

ABSTRACT

In this study, new composite adsorbent with enhanced thermal conductivity and adsorption capacity was synthesized and analyzed comprehensively for the development of compact CO_2 based adsorption cooling system. The consolidated composite was prepared employing activated carbon, graphene nanoplatelets and hydroxyl cellulose as a parent adsorbent, thermal conductivity enhancer, and binder, respectively. The surface area and pore volume of the composite were found to be 1778 ± 13 m^2 g^{-1} and 1.014 cm^3 g^{-1}, respectively. In addition, the composite showed 233% higher thermal conductivity compared to the parent activated carbon. Adsorption characteristics of CO_2 were measured at temperature ranging from 20 to 70 °C and pressures up to 5 MPa. Absolute uptake was evaluated from excess adsorption based on the following two methods: (i) the adsorbed phase volume is equal to the pore volume of the adsorbent; and (ii) the adsorbed phase volume is almost zero under low pressure and/or high temperature conditions. Furthermore, the averaging of above two methods was also taken for avoiding these two extreme assumptions. Obtained absolute adsorption uptake data were fitted with modified Dubinin-Astakhov and Tóth models. Results indicated good approximation between data points and models. The average isosteric heats of adsorption estimated using modified D-A and Tóth model were found to be 19.742 kJ mol^{-1} and 19.023 kJ mol^{-1}, respectively. The obtained characteristics of composite adsorbent are prerequisites for designing compact CO_2 based adsorption cooling systems.

Une étude complète visant à mesurer l'absorption absolue de dioxyde de carbone sur un adsorbant composite

Mots-clés: Adsorption; Absorption absolue; Composite; Modèle isotherme; Conductivité thermique

1. Introduction

The process of adsorption of gases has been used in various application, for instances: gas storage (Sahoo and Ramgopal, 2016; Singh and Kumar, 2017a; Zakaria and George, 2011); cooling systems (Fan et al., 2016; Jribi et al., 2014; Lemmini and Errougani, 2005; Pal et al., 2016c); and CO_2 capture and sequestration (Rezaei

* Corresponding author at: International Institute for Carbon-Neutral Energy Research (WPI-I2CNER), Kyushu University, 744 Motooka, Nishi-ku, Fukuoka 819-0395, Japan.
E-mail address: saha.baran.bidyut.213@m.kyushu-u.ac.jp (B.B. Saha).

https://doi.org/10.1016/j.ijrefrig.2019.01.014
0140-7007/

Nomenclature

A	adsorption potential [J mol^{-1}]
b_0	equilibrium constant [kPa^{-1}]
C	amount adsorbed [g g^{-1}]
C_0	saturated amount adsorbed [g g^{-1}]
E	characteristic energy [J mol^{-1}]
ΔH_0	isosteric heat of adsorption [J mol^{-1}]
k	fitting parameter [-]
m	structural heterogeneity parameter [-]
n_{abs}	absolute molar uptake [mmol g^{-1}]; $n_{abs} = q_{abs} \cdot M(CO_2)$
n_{excess}	excess molar uptake [mmol g^{-1}]; $n_{excess} = q_{excess} \cdot M(CO_2)$
P	equilibrium pressure [kPa]
P_s	saturation pressure [kPa]
P_c	critical pressure [kPa]
q_{abs}	absolute mass uptake [g g^{-1}]
q_{excess}	excess mass uptake [g g^{-1}]
Q_{st}	isosteric heat of adsorption [kJ mol^{-1}]
R	universal gas constant [J mol^{-1} K^{-1}]
S	specific surface area [m^2 g^{-1}]
t	heterogeneity parameter [-]
T	temperature [K]
T_c	critical temperature [K]
T_t	triple point temperature [K]
ν_{pore}	pore volume [cm^3 g^{-1}]
V_a	adsorbed phase volume [cm^3 g^{-1}]
V_t	molar volume of gas at triple point [cm^3 g^{-1}]
W	volumetric adsorption uptake [cm^3 g^{-1}]
W_0	limiting micropore capacity [cm^3 g^{-1}]
z_b	adsorption space thickness [m]

Greek symbols

α	thermal expansion of the adsorbed gas [K^{-1}]
θ	surface coverage, is equal to $\theta = C/C_0$
ρ_b	bulk gas density [g cm^{-3}]

and Webley, 2010; Saxena et al., 2014; Singh and Kumar, 2015). Zakaria and George (2011) mentioned that during adsorption storage of methane, the pressure in the storage tank is reduced up to 5 times compared to the compression storage. Authors illustrated it regarding the capacity of empty tank and adsorbent filled tank, and showed that the energy density of the adsorbent filled tank was 5 times higher than that of empty tank at 3.5 MPa. Therefore the adsorption storage is widely used in gaseous fuel driven vehicles because of its safeness. At the same time, adsorption gas cylinders do not require the use of an expensive preliminary multistage compression tool. This makes adsorption gas cylinders less explosive and hazardous. In an adsorption heating or cooling system, the electrically powered compressor of conventional compression based system is replaced by thermally driven adsorber/desorber heat exchangers. Therefore, adsorption cooling/heating systems are fully functional without electricity supply (Chahbani et al., 2004) which allows the use of this technology in remote regions having zero access to electricity. The solar energy or the waste heat can be utilized as a source of energy for the adsorption cooling systems operation (Gwadera and Kupiec, 2011; Kadam et al., 2016).

In adsorption cooling systems (ACS), natural substances like carbon dioxide (CO_2), water, methanol, ethanol, ammonia are used as a refrigerant. CO_2 is a promising refrigerant because it provides numerous benefits including high volumetric capacity and availability. Furthermore, it is a nonflammable, non-toxic refrigerant having zero ODP and GWP (=1) (Pal et al., 2016c). Adsorption uptake is one of the key parameters and fundamental characteristics to determine the performance of ACS. However, there is no equipment that can make direct measurement of absolute adsorption of CO_2 and also other high pressure gasses such as CH_4, R32 and N_2 (Shen et al., 2010). Experimental measurements usually provide the excess adsorption value. During the adsorption process, pore volume is partially occupied by the adsorbate molecules in the adsorbed state and partially with molecules in free molecular phase. According to the Gibbs definition, absolute uptake is the amount of gas molecules that are in the adsorbed state in a porous material. Sometimes all the adsorbate molecules entering through the envelope of the adsorbent particles is considered as absolute uptake, no matter whether the molecule is in the adsorbed or free gas state. The precise estimation of absolute adsorption uptake from excess adsorption is critical since it requires the value of either the density or the specific volume of adsorbed gas, which are very difficult to determine as they are functions of temperature and pressure. The theory to evaluate absolute uptake includes many assumptions such as (Tóth, 2002):

(1) Assuming the density of the adsorbed phase is equal to the density of the saturated liquid.
(2) Considering the adsorbed phase as closely packed molecules at a specified diameter, usually corresponds to the van der Waals volume.
(3) Evaluating the adsorbed phase density based on the linear section of the excess adsorption versus bulk density plot.
(4) Assuming the volume of the adsorbed phase equal to that of pores.

Shen et al. (2010) measured the adsorption of CO_2 onto activated carbon (AC) beads employing gravimetric method. To obtain the absolute adsorption, authors corrected the measured excess adsorption using the above mentioned assumption 1. Jribi et al. (2017) investigated the adsorption isotherms and kinetics of CO_2 onto AC powder of type Maxsorb III using gravimetric method. To obtain the absolute adsorption, the measured excess adsorption data are corrected using the above mentioned assumption 4. Processing of experimental results differs depending on the techniques used for the adsorption measurement: volumetric or gravimetric (Myers and Monson, 2014).

Recently, scientists are working on how to make ACS more compact and efficient by development of composite adsorbent material possessing enhanced thermal conductivity and volumetric uptake (Askalany et al., 2017; El-Sharkawy et al., 2016; Jin et al., 2013; Pal et al., 2019; Wang et al., 2011). In this study, consolidated composite adsorbent is synthesized with a composition ratio of 50 wt% activated carbon (Maxsorb III), 40 wt% graphene nanoplatelets, 10 wt% hydroxyl cellulose for enhancing the thermal conductivity as well as volumetric adsorption uptake. Porous properties and thermal conductivity of synthesized composite are investigated. In addition, adsorption characteristics of CO_2 onto composite are observed for adsorption temperature ranging from 20 to 70 °C up to 5 MPa thermogravimetrically using magnetic suspension adsorption measurement apparatus. The present work also discusses comprehensive study for evaluating accurate absolute adsorption uptake. Obtained absolute adsorption data are fitted to modified D-A and Tóth isotherm models to find the isotherm parameters and heat of adsorption.

2. Experiments

2.1. Synthesis of composite

In this study, we synthesized consolidated activated carbon (Maxsorb III) composite adsorbent using graphene nanoplatelets (C750) and hydroxyl cellulose (HEC) as a binder. The composition ratios were 50 wt% Maxsorb III, 40 wt% C750, and 10 wt% HEC for

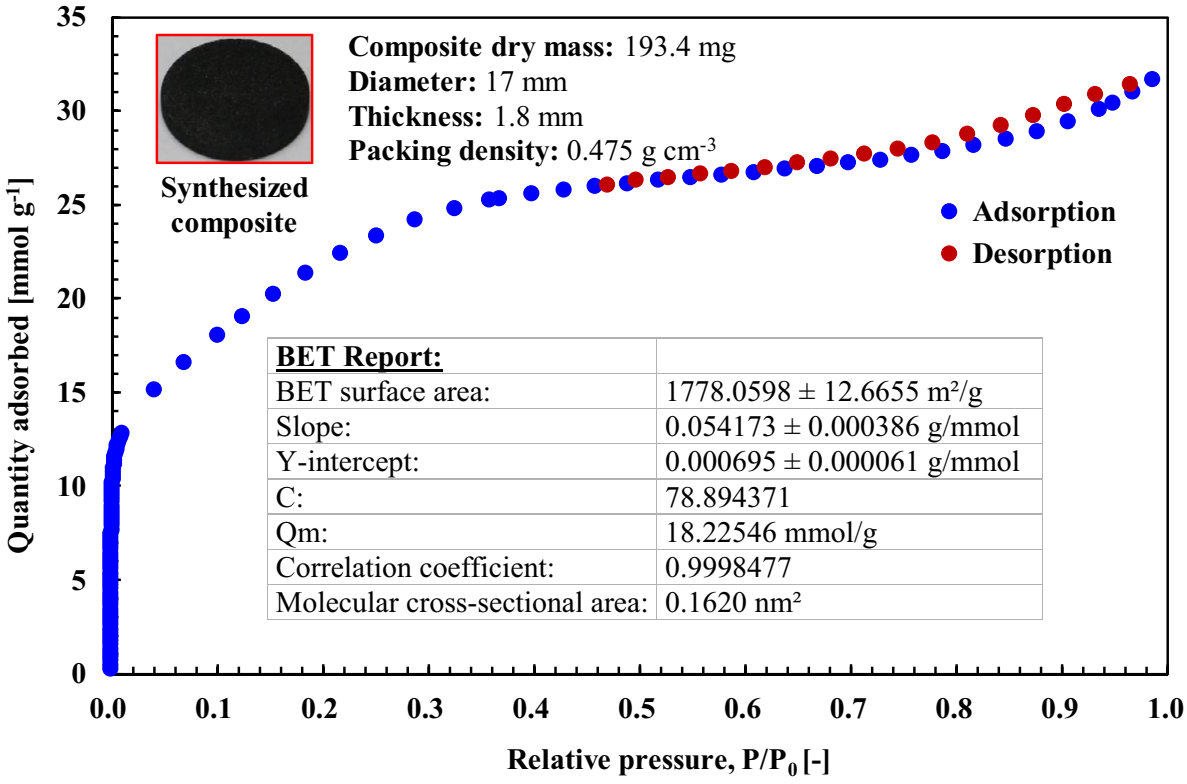

Fig. 1. N_2 adsorption and desorption isotherms onto composite.

enhanced the thermal conductivity as well as volumetric adsorption uptake. The synthesis procedure can be explained as follows (El-Sharkawy et al., 2016; Pal et al., 2017, 2016a, b, c), at first, Maxsorb III and C750 were dried in an oven at 150 °C for several hours to remove the moisture content and minimize the weight measurement error. The binder HEC is of granular type. To make the HEC solution, water was added into the binder. After that Maxsorb III and C750 were mixed and put into the binder solution. The mixer was compressed using a mechanical compressor. Finally, the composite sample was dried in the oven at 120 °C for several hours to remove the water content. After that, the same composite is used for characterization such as porous properties, thermal conductivity, and CO_2 adsorption characteristics. The photograph and physical properties of the synthesized composite are presented in Fig. 1.

2.2. Characteristic results of composite

Nitrogen (N_2) adsorption onto the adsorbent is one of the standard methods to determine the porous properties such as specific surface area, pore volume and pore size distribution of adsorbent material (Pal et al., 2019). The N_2 adsorption/desorption isotherm of the synthesized composite was investigated using the volumetric method employing 3Flex™ Surface Characterization Analyzer supplied by Micromeritics, Japan. In this experiment, a pressure transducers accuracy of 0.15% of the reading with a resolution to 10^{-5} mmHg was employed to measure the pressure of N_2 adsorption gas. The measurement error range was automatically calculated by the analyzing software given by 3Flex manufacturer and always shown in BET surface area value. N_2 adsorption/desorption experiment was conducted at −196 °C (77 K) after a regeneration temperature at 250 °C for several hours. Fig. 1 shows the N_2 adsorption/desorption isotherm onto studied composite. It can be seen that there is no hysteresis which is important for adsorption heat pump applications. Characteristics of this figure ascertains that the composite is mostly microporous. Brunaure–Emmett–Teller (BET) method with multi-point surface area analysis was adopted to calculate the surface area. It is observed that the composite possesses BET surface area of 1778 ± 13 m^2 g^{-1}.

The pore-size distribution (PSD) analysis was carried out using the Non-Local Density Functional Theory (NLDFT) by applying the provided software package of 3Flex. Fig. 2 shows the cumulated pore volume and PSD analysis of the composite adsorbent. It is observed that the total pore volume of composite is 1.014 cm^3 g^{-1}. The surface area and pore volume of the present study along with published data of various carbon based adsorbents are enlisted in Table 4.

The thermal conductivity of the synthesized composite adsorbent was measured using NETZSCH LFA 457 MicroFlash system. The details of instrument and measurement procedure of thermal conductivity can be found elsewhere (El-Sharkawy et al., 2016; Pal et al., 2019). The thermal diffusivity can be measured by this instrument with an accuracy and repeatability of ±3% and ±2%, respectively. The composite thickness was 1.8 mm, measured using QuantuMike micrometer with resolution of 0.001 mm and instrumental error of ±1 μm. The measurement was conducted at room temperature and atmospheric pressure conditions. The thermal diffusivity of composite was measured six times and the standard deviation for the measured data was calculated and found as ± 0.01. The studied composite possesses thermal diffusivity and thermal conductivity of 0.564 ± 0.01 mm^2 s^{-1} and 0.22 W m^{-1} K^{-1}, respectively. It should be noted that composite shows 233% higher thermal conductivity compared to parent adsorbent.

2.3. Adsorption uptake measurement

The magnetic suspension balance unit (MSB-GS-100-10 M) supplied by MicrotracBEL, Japan was used to measure the adsorption isotherms of CO_2 onto composite. A detailed description of this instrument can be found in references (Jribi et al., 2017;

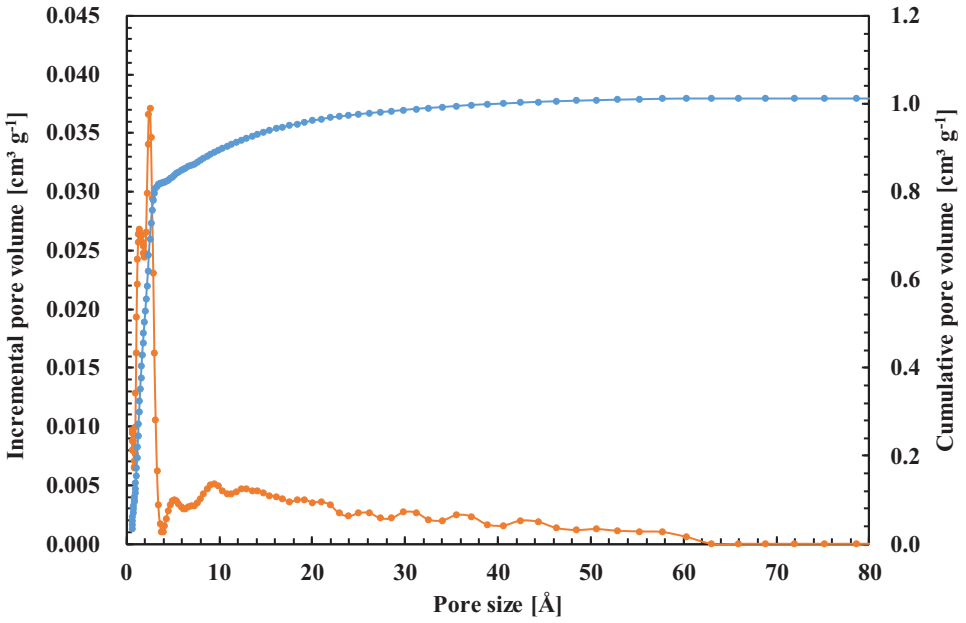

Fig. 2. PSD analysis of composite.

Pal et al., 2016c). It consists of a magnetic suspension balance unit; an evaporator; isothermal circulation oil bath to control the adsorption/evaporation temperatures; isothermal air bath to avoid condensation within the system; and a series of vacuum pumps including rotary, diaphragm and turbo-molecular pump. One absolute pressure gauge of 10,000 kPa, Keller PAA-35X is used to measure the pressure of CO_2 gas with an uncertainty of ±0.1 of full scale. The system contains a platinum temperature element (Pt 100 Ω) to control and measure the temperature of the sample section. It is connected to the Julabo (type: F25-ME) circulation oil bath and the measurable temperature range is −10–200 °C. Measurement procedure can be described as follows; firstly, the consolidated composite adsorbent of amount 193.4 mg was put into the sample container and connected to the measuring unit of the system. After that, the leak test was performed. The sample was then heated at 130 °C for several hours under vacuum condition for each isotherm to remove any adsorbed gas. Then the temperature was stabilized for measurement condition. Measurements were conducted at six different adsorption temperatures ranging from 20 to 70 °C with pressure up to 5 MPa for each temperature. The whole experiment was executed automatically by the instruction given in software. The sample weight was directly measured by magnetic suspension balance with ±1 μg resolution. Mass measurement repeatability of magnetic balance is ±30 μg with relative error of ±0.002% of the reading. Since the composite mass used in the study was about 193.4 mg, the relative experimental error was always less than 0.002%.

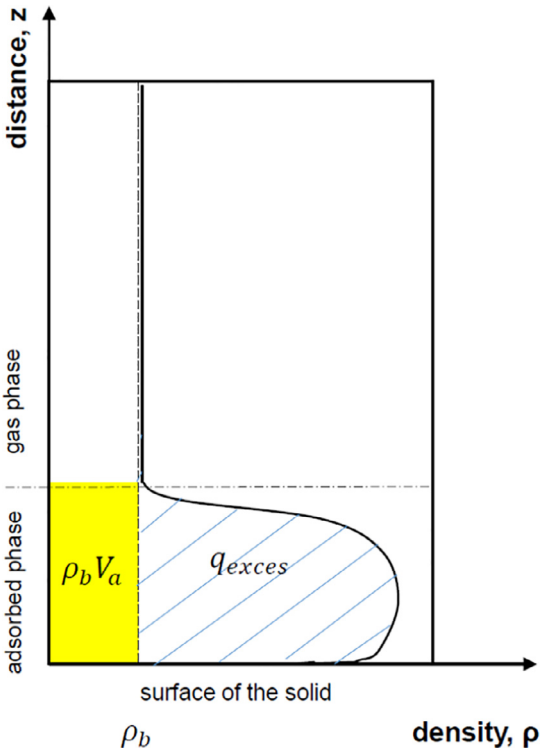

Fig. 3. Schematic illustration of adsorption process. Dependency of adsorbate density on the distance from the solid surface (Tóth, 2002).

3. Absolute adsorption uptake estimation

In Fig. 3 the solid line shows the dependency of adsorbate density as a function of the distance from the surface (Tóth, 2002). During adsorption, the density of adsorbate molecules has higher value within the small distance from the solid surface because gas molecules at adsorbed phase are packed densely. The thickness of the adsorption space, z_b, depends on the number of adsorbate layers. Above adsorption space, the density of gas is equal to the bulk density, ρ_b. So, assuming uniform adsorption and by treating the 3D solid-gas interface as an imaginary mathematical surface, the absolute adsorption, is found as follows:

$$q_{abs} = S\int_0^{z_b} \rho(z)dz \tag{1}$$

The experimental data measured by gravimetric apparatus (TGA) gives lower value of adsorption uptake than the value really enclosed in the adsorbent sample, because the sample is weighted while immersed in bulk gas, and pushed up by Archimedes' force, equal to the weight of gas displaced by the skeletal volume of the adsorbent sample and adsorbed phase volumes. Therefore,

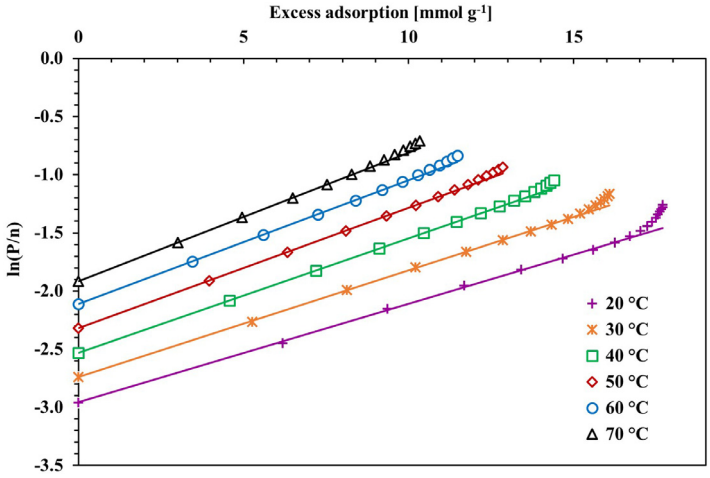

Fig. 4. Virial plot of adsorption data.

corrections for both the skeletal volume of the sample and the volume of the adsorbed phase must be done in order to find the correct absolute adsorption values. The TGA apparatus does the buoyancy correction for skeletal volume before providing the data, therefore, it gives excess adsorption. The excess adsorption corresponds to the shaded area in Fig. 3, and evaluated as:

$$q_{excess} = S\int_0^{\infty} (\rho(z) - \rho_b)dz \tag{2}$$

or

$$q_{excess} = S\int_0^{z_b} (\rho(z) - \rho_b)dz \tag{3}$$

As for $z \geq z_b$ the gas density $\rho\ (z) = \rho_b$. Therefore, the absolute adsorption can be found by adding the product of the bulk density and the adsorbed phase volume to the value of excess adsorption. The absolute adsorption here is the number of moles of gas contained in all the accessible pore volume of the porous material. The adsorbed phase volume, V_a, is the product of the adsorption space thickness, z_b, and the specific surface area, S.

$$q_{abs} = q_{excess} + \rho_b \cdot V_a \tag{4}$$

$$V_a = S \cdot z_b \tag{5}$$

At supercritical regimes, the volume of the adsorbed phase V_a becomes negligible because the strength of gas–gas interaction is very weak and only single layer adsorption is possible on the wall. That is why excess and absolute adsorption uptake in supercritical regimes do not deviate much as in sub-critical regimes.

In this study two methods for the evaluation of the absolute uptake are considered: (a) the specific volume of gas in the adsorbed state is equal to the specific pore volume (Pal et al., 2016c); (b) assuming that the absolute uptake is equal to excess uptake, or V_a is almost zero under low pressure and/or high temperature conditions (Zhou et al., 2003; Zhou and Zhou, 1998, 1996). The details of these methods are explained in the following sections.

3.1. Absolute adsorption estimation using the first method

According to the first method, $V_a = V_{pore}$, the absolute adsorption uptake can be found from excess adsorption using the following equation.

$$q_{abs} = q_{excess} + \rho_{CO_2} \cdot V_{pore} \tag{6}$$

Table 1
Evaluated Henry constants.

Temperature [K]	Intercept	K	ln K
293.15	−2.956	19.22093405	2.956
303.15	−2.7402	15.4900828	2.7402
313.15	−2.5317	12.57486525	2.5317
323.15	−2.3199	10.17465679	2.3199
333.15	−2.1131	8.273850506	2.1131
343.15	−1.9172	6.801886499	1.9172

3.2. Absolute adsorption estimation using the second method

According to the second method, firstly the experimental excess adsorption uptake data are constructed in terms of ln (P/n) versus n excess adsorption, which is called the virial form of the adsorption data and illustrated in Fig. 4.

The curves have a linear form at low surface concentrations, which is used in the evaluation of Henry constants $K(T)$. The obtained values of Henry constant for different temperatures are presented in Table 1.

The plot of Henry constants versus temperature in terms of ln (K) versus $1/T$ is known as *van't Hoff plot*, and for the adsorbent–adsorbate pair under consideration it shows linear dependency. Thus the Henry constants can be derived as a function of temperature. The best-fit straight line with an accuracy value of approximation $R^2 = 0.9989$ is as following:

$$K = \exp\left(-4.1703 + \frac{2093.7}{T}\right) \tag{7}$$

$$K = K_0\ \exp\left(-\frac{\Delta H_0}{RT}\right) \tag{8}$$

The advantage of the second method is that it allows the evaluation of the isosteric heat of adsorption (enthalpy or also referred to as limiting heat of adsorption) at this stage, using Eq. (9). From the log-log plot of K versus $1/T$ the isosteric heat of adsorption is found to be $\Delta H_0 = -17.407$ kJ mol^{-1} (i.e. 395.53 kJ kg^{-1}) and $K_0 = 0.0154$.

$$\frac{d\ln K}{dT} = \frac{\Delta H_0}{RT^2} \text{ or slope} = \frac{d\ln K}{d\left(\frac{1}{T}\right)} = -\frac{\Delta H_0}{R} \tag{9}$$

Let, $K{\cdot}P$ be the product of the Henry constant and the pressure. Fig. 5 illustrates the comprehensive adsorption curve in terms of ln $(K{\cdot}P)$ versus ln (n), where all isotherms reduce to a single general-

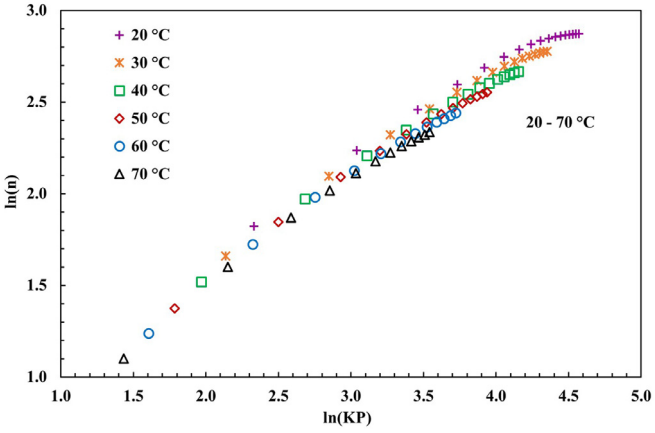

Fig. 5. Comprehensive adsorption curve.

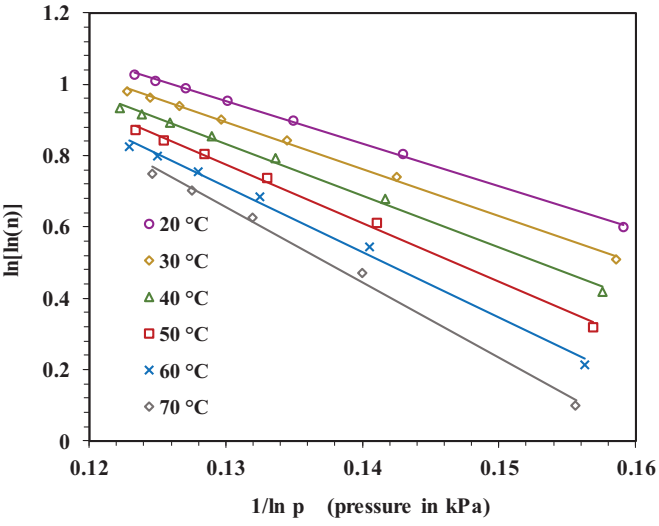

Fig. 6. Second linearized transformation of adsorption isotherms.

Table 2
Values of α and β at different temperatures.

Temperature [K]	α	β
293.15	2.4952	−11.868
303.15	2.6039	−13.157
313.15	2.7237	−14.543
323.15	2.9133	−16.446
333.15	3.1048	−18.393
343.15	3.3953	−21.086

ized curve. Linear section of the comprehensive adsorption curve corresponds to the low surface coverage.

Data points corresponding to low surface concentrations are used for estimation of absolute uptake. Second linearization transformation is done by the representation of adsorption isotherms in ln (ln n) versus 1/ln P coordinates as shown in Fig. 6, from where the values of slope (β) and intercept (α) of each line found and used in construction of generalized absolute adsorption model. Obtained values of α and β are given in Table 2.

The values of α and β can be found as a function of temperature,

$$\alpha(T) = 0.0177 * T - 2.7566 \tag{10}$$

$$\beta(T) = -0.182 * T + 41.989 \tag{11}$$

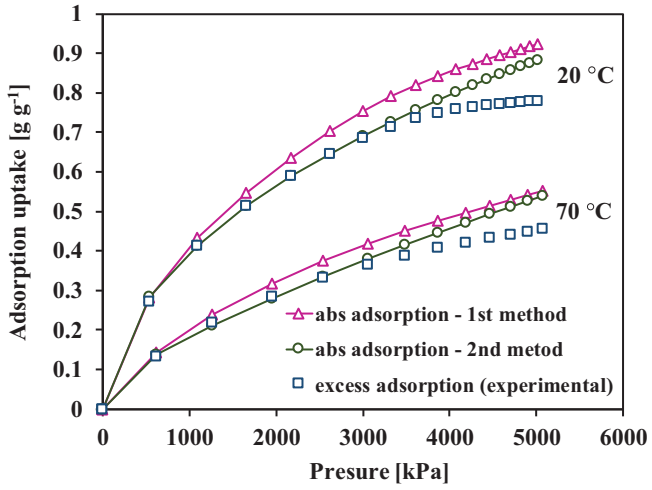

Fig. 7. Experimental excess uptake versus absolute uptake estimated according to the first and second methods.

As a result, the generalized absolute adsorption model according to the second method is described by the below equations,

$$\ln[\ln n] = \alpha(T) + \frac{\beta(T)}{\ln P} \tag{12}$$

or

$$n_{abs} = \exp\left[\exp\left(\alpha(T) + \frac{\beta(T)}{\ln P}\right)\right] \tag{13}$$

Absolute adsorption values calculated using the methods discussed in Sections 3.1 and 3.2 are illustrated in Fig. 7. In the figure, only 20 °C and 70 °C isotherms are shown. As can be seen from Fig. 7, while using the first method the absolute uptake always exceeds experimental excess adsorption, whereas in the second method absolute and excess adsorption data overlap at lower pressure values. The first method assumes the adsorbed phase volume is equal to the pore volume, $V_a = V_{pore}$, which means that the case considers all the adsorbate molecules entering through the envelope of the adsorbent sample (through the shell of the sample) as an absolute uptake; this assumption gives higher value for volumetric uptake. However, in the second method, absolute uptake is considered as the amount of molecules that are in the adsorbed state in the sample. Therefore, the molecules in the pore volume, which are in the free gas phase (not in the adsorbed state), are not taken into account. This is implemented through the assumption that under low pressure and/or high temperature conditions the adsorbed phase volume is almost zero, $V_a = 0$ (when $P \to 0$ and/or $T \to \infty$). Therefore, the excess uptake can be considered as absolute uptake and the curves are overlapped at this region.

3.3. Proposed method: averaging the two methods

Above mentioned two absolute uptake estimation methods can be referred as two extreme assumptions, and allow to know the upper and lower limits of possible absolute uptake. Ideally, the absolute adsorption uptake is found by adding the excess uptake to the mass of gas contained in the adsorbed phase volume, V_a, (Eq. (4)). The true absolute adsorption uptake value is somewhere in-between the data obtained using both methods, therefore the average should give the best closest fit.

$$q_{abs}^{ave} = \frac{q_{abs}^{I} + q_{abs}^{II}}{2} \tag{14}$$

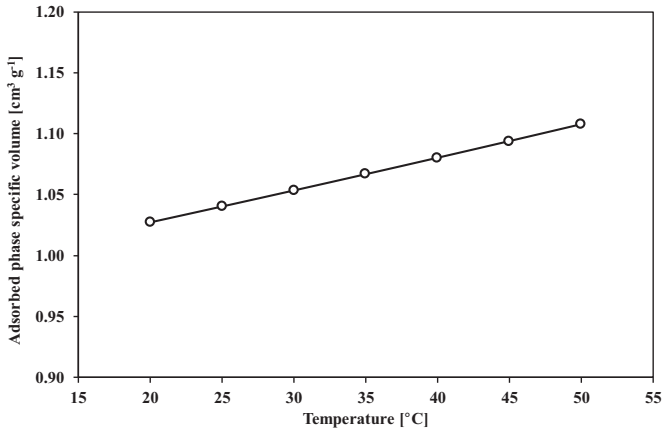

Fig. 8. Temperature dependence of adsorbed phase specific volume.

4. Adsorption isotherm models

Absolute adsorption data obtained by application of two main methods and the average of them are fitted to modified D-A and Tóth models. Modified Dubinin–Astakhov model can be expressed as (Eqs. (15)–(18) (Jribi et al., 2017; Pal et al., 2016c).

$$q_{abs} = \frac{W_0}{V_m} \exp\left(-\left(\frac{A}{E}\right)^m\right) \tag{15}$$

Where,

$$A = RT\ln\left(\frac{P_s}{P}\right) \tag{16}$$

$$P_s = \left(\frac{T}{T_c}\right)^k P_c \tag{17}$$

$$V_m = V_t \exp\left(\alpha(T - T_t)\right) \tag{18}$$

where, W_0 is the limiting micropore volume [cm^3 g^{-1}], A is the adsorption potential [J mol^{-1}], E is the characteristic energy [J mol^{-1}], m is the structural heterogeneity parameter [-], T_c and P_c are the critical temperature [K] and pressure [kPa], respectively, T_t is the triple point temperature [K], V_t is the molar volume of liquid carbon dioxide at triple point which is 0.84858 cm^3 g^{-1}, α is the thermal expansion which is 0.0025 K^{-1} (Pal et al., 2016c). k is the exponent for calculating the saturation pressure above critical temperature. If $k=2$, Eq. (15) is called classical D-A model (Amankwah and Schwarz, 1995; Singh and Anil Kumar, 2016), otherwise it is called modified D-A model (Pal et al., 2016c). V_m is the molar volume of adsorbed phase [cm^3 g^{-1}]. The variation of V_m with adsorption temperature is shown in Fig. 8. It needs mentioning that the adsorbed phase specific volume is a specific property of an adsorbent–adsorbate pair and cannot be generalized (Srinivasan et al., 2011). In the current study, V_m increases with the rise in temperature.

Tóth model is expressed by the below equation

$$\frac{C}{C_0} = \frac{b_0 e^{\frac{Q_{st}}{RT}} P}{\left(1 + \left(b_0 e^{\frac{Q_{st}}{RT}} P\right)^t\right)^{1/t}} \tag{19}$$

where C is the amount adsorbed [g g^{-1}], C_0 is the saturated amount adsorbed [g g^{-1}], Q_{st} is the isosteric heat of adsorption [kJ mol^{-1}], b_0 is the equilibrium constant [kPa^{-1}], P is the equilibrium pressure [kPa]. Root-mean-square deviation (RMSD) is used as a measure of prediction error,

$$RMSD = \sqrt{\frac{\sum_{i=1}^{n}\left(\hat{y}_i - y_i\right)^2}{n}} \tag{20}$$

Table 3
Parameters for global modified D-A and Tóth isotherm models fitted to the absolute uptake evaluated according to the first and second method and by averaging method.

Estimated parameters	1st method	2nd method	Averaging method
Modified D-A model			
k [-]	4.56441	4.14575	4.365462
E [J mol^{-1}]	5068.48	4703.68	4900.28
m [-]	1.141005	1.06136	1.103914
W_0 [cm^3 g^{-1}]	1.02570	1.00814	1.01487
RMSD [%]	0.791	0.751	0.621682
Tóth model			
C_0 [g g^{-1}]	2.714573	2.548024	2.630838
b_0 [kPa^{-1}]	1.88922E−07	1.8892E−07	1.8892E−07
Q [kJ mol^{-1}]	19.026	19.021	19.024
t [-]	0.477183	0.477179	0.477317
RMSD [%]	0.366	1.0647	0.5644

Fig. 9(a) and (b) represent the graphical illustration of the results of fitting absolute adsorption data obtained by two main methods with modified D-A and Tóth models. It is observed that both isotherm models fit well with absolute uptake calculated using 1st and 2nd methods. However, Tóth model is better for 1st interpretation whereas modified D-A is better for 2nd interpretation. Averaged Tóth model shows low RSMD value compared to averaged modified D-A model. Isotherm parameters and RMSD values of both models are shown in Table 3. The maximum uptake of composite/CO_2 pair is found to be 1.02 cm^3 g^{-1} and 2.71 g g^{-1} for modified D-A and Tóth model, respectively. The power k, from modified D-A model, for setting pseudo vapor saturation pressure (Amankwah and Schwarz, 1995), is comparable with the one obtained for CO_2 adsorption onto another AC studied (Jribi et al., 2017), where the value is found to be $k=4.504$. Graphical comparison of all three methods are illustrated in Fig. 10(a) and (b) in terms of modified D-A and Tóth model, respectively. The maximum adsorption uptake of CO_2 onto various conventional carbon based adsorbents reported in literature is presented in Table 4 and compared with present study.

5. Isosteric heat of adsorption

The isosteric heat of adsorption (Q_{st}) is an important property of any adsorbent/adsorbate pair because it signifies that whether a particular pair is good for adsorption refrigeration or heating applications. The values of Q_{st} depends on the adsorbent/adsorbate pair. Higher value of Q_{st} means good for heating applications whereas lower value indicates for refrigeration/cooling applications (Srinivasan et al., 2012). Tóth equation includes isosteric heat of adsorption Q_{st} as a fitting parameter which is defined during correlation stage. Therefore, the value of Q_{st} is constant and doesn't depend on the surface coverage. However, when the isosteric heat of adsorption derived from modified D-A model, it is found as a function of surface coverage, $\theta = C/C_0$. Clausius–Clapeyron (C–C) equation, Eq. (21), is used to establish the dependency between the surface coverage θ and isosteric heat of adsorption Q_{st} (Rahman et al., 2013).

$$Q_{st} = RT^2\left(\frac{\partial \ln P}{\partial T}\right)_{\text{const }\theta} = R\left(\frac{\partial \ln P}{\partial\left(\frac{1}{T}\right)}\right)_{\text{const }\theta} \tag{21}$$

The C–C plot is constructed via reverse calculation of pressure for varying temperatures at constant surface coverage θ via below

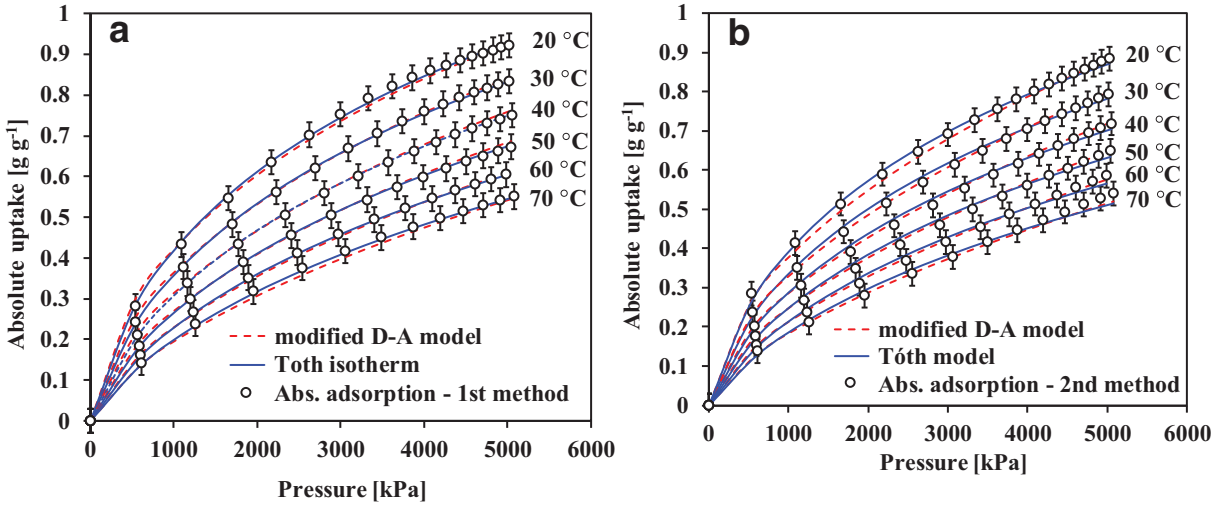

Fig. 9. Modified D-A and Tóth isotherm models fitted with the absolute uptake estimated using the (a) first method and (b) second method with ± 5% error bars in uptake.

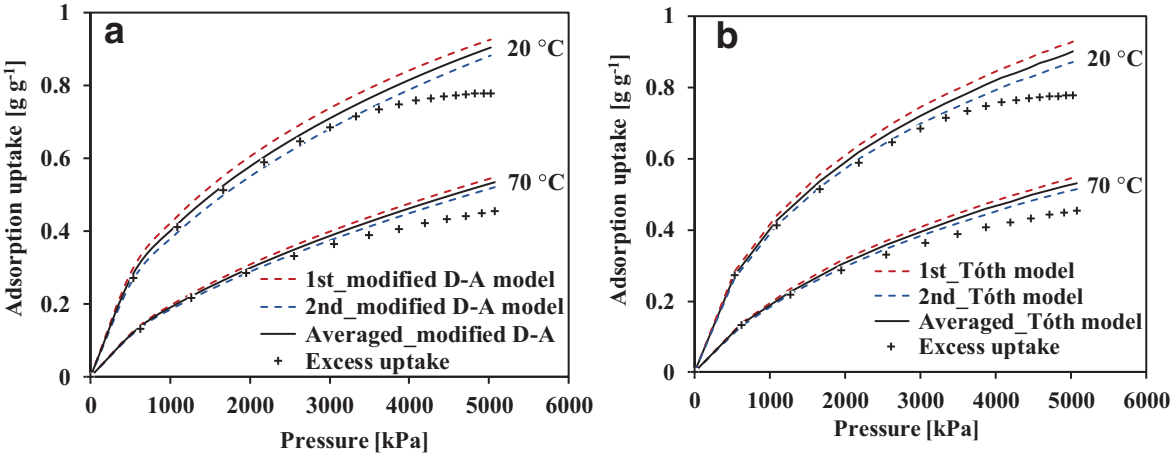

Fig. 10. (a) Modified D-A; (b) Tóth isotherm models along with experimental excess adsorption uptake.

Table 4
Comparison of maximum CO_2 uptake, isosteric heat of adsorption, surface area, pore volume and thermal conductivity of different adsorbents.

Adsorbent/CO_2	Maximum uptake (using modified D-A model), W_0 [cm^3 g^{-1}]	Isosteric heat of adsorption, Q_{st} [kJ mol^{-1}]	Surface area [m^2 g^{-1}]	Pore volume [cm^3 g^{-1}]	Thermal conductivity [W m^{-1} K^{-1}]	Reference
Composite	1.015	19.023	1778	1.014	0.22	Present study
Maxsorb III	1.5408	19.30	3045	1.70	0.066	(El-Sharkawy et al., 2016; Jribi et al., 2017)
A-20 (ACF)	1.03	19.23	2000	1.03	–	(Saha et al., 2011)
Composite	1.109	22.5	2000	1.094	0.24	(Pal et al., 2016c)
Norit R1 Extra	0.67	22.0	1450	0.47	–	(Himeno et al., 2005)
BPL	0.51	25.7	1150	0.43	–	(Himeno et al., 2005)
A10 fiber	0.54	21.6	1200	0.59	–	(Himeno et al., 2005)
Activated carbon A	0.55	17.8	1207	0.54	–	(Himeno et al., 2005)
Norit RB3 (AC1)	1.09	15.51	987.04	0.51	–	(Singh and Kumar, 2017b)
Norit Darco (100 mesh size) (AC2)	0.898	16.27	876.45	0.73	–	(Singh and Kumar, 2017b)
Norit Darco (12 × 20 US mesh size) (AC3)	0.62	16.53	462.67	0.50	–	(Singh and Kumar, 2017b)
CSAC	0.55	16.44	804.02	0.43	–	(Singh et al., 2018; Singh and Kumar, 2017c)

equation.

$$\ln P = \ln\left[\left(\frac{T}{T_c}\right)^k P_c\right] - \frac{E}{RT}\sqrt[m]{\ln\frac{W_0}{CV_t \exp\left(\alpha(T-T_t)\right)}} \tag{22}$$

Fig. 11(a) shows C–C plot constructed in terms of $\ln p$ versus $1/T$ from generalized modified D-A model. Tangential of each line corresponding to constant uptake linearly depends on the isosteric heat of adsorption, Eq. (21). Comparison of isosteric heat of adsorption values estimated from Tóth and modified D-A models are plotted in Fig. 11(b). Average value of Q_{st} estimated using modified D-A model is 19.742 kJ mol^{-1}, and using Tóth model is 19.023 kJ mol^{-1}. In these calculations, the adsorbate is assumed to behave like a perfect gas. The heat of adsorption value of the synthesized composite/CO_2 pair is having close resemblance with other conventional carbon based adsorbent/CO_2 pairs, which is given in Table 4.

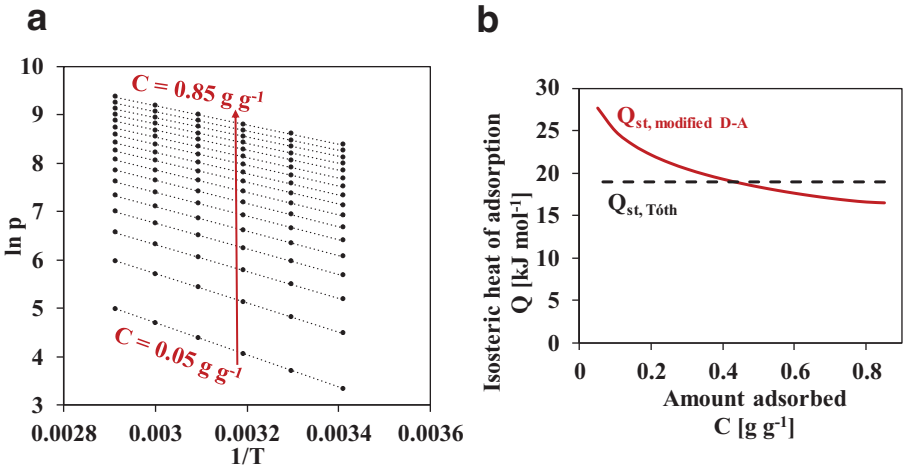

Fig. 11. (a) Clausius–Clapeyron (C–C) plot constructed using modified D-A model; (b) Isosteric heat of adsorption versus adsorption uptake.

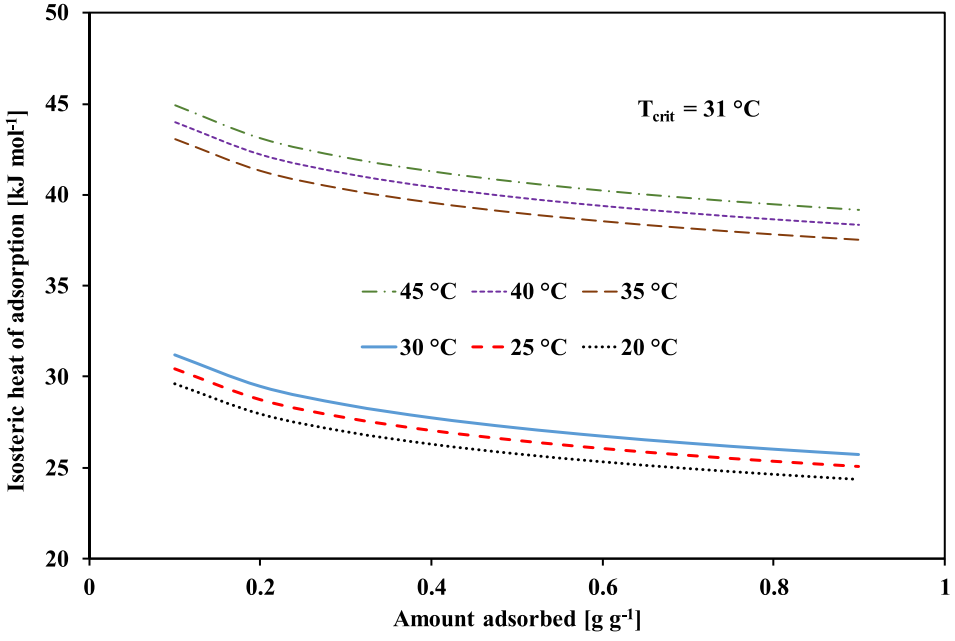

Fig. 12. Dependence of isosteric heat of adsorption on adsorption uptake.

However, the perfect gas assumption in estimating the heat of adsorption using Clausius–Clapeyron equation is only valid at low pressure and may result in significant errors for high pressure adsorption applications. Even at partial vacuum adsorption, Shen et al. (2000) observed a discrepancy of around 2 kJ mol^{-1} between the calorimetry method predictions by the Clausius–Clapeyron equation. Rahman et al. (2013) proposed Eqs. (23) and (24) to measure Q_{st} at pressures lower and higher than critical pressures respectively. The results are presented in Fig. 12.

$$Q_{st} = h_{fg} + E\left\{(-\ln\theta)^{\frac{1}{n}} + \frac{T\alpha}{n}(-\ln\theta)^{\frac{1}{n}-1}\right\} \quad (23)$$

$$Q_{st} = kRT + E\left\{(-\ln\theta)^{\frac{1}{n}} + \frac{T\alpha}{n}(-\ln\theta)^{\frac{1}{n}-1}\right\} \quad (24)$$

It is observed that Q_{st} decreases with increase in uptake and at temperatures higher than T_c, the heat of adsorption value is much higher. Similar trend is also found in literature (Azahar et al., 2018).

6. Conclusions

The developed consolidated composite adsorbent for potential application in CO_2 based cooling systems demonstrated enhanced thermal conductivity, which was 233% higher than that of parent adsorbent. Composite showed specific BET surface area of 1778 ± 13 m^2 g^{-1} and total pore volume of 1.014 cm^3 g^{-1}. Magnetic suspension adsorption measurement apparatus was employed to measure the adsorption characteristics of composite/CO_2 pair for a wide range of temperatures and pressures. Absolute adsorption uptake was estimated from excess adsorption uptake in two steps:

(1) In the first step, the absolute uptakes were estimated using two different assumptions, that also can be referred as two extreme cases: (i) the adsorbed phase volume is equal to the pore volume, $V_a = V_{pore}$, and (ii) the adsorbed phase volume is almost zero under low pressure and/or high-temperature conditions, $V_a = 0$ (when $P \to 0$ and/or $T \to \infty$).

(2) After that, the averaging of above two methods was also taken for avoiding these extreme assumptions and used in further analysis.

Obtained data were fitted to modified Dubinin-Astakhov (D-A) and Tóth isotherm models; thereby generalized isotherm models were constructed. Correlation errors for modified D-A and Tóth models in terms of the RMSD were 0.62% and 0.56%, respectively, which indicates a good approximation of data points. From the Tóth model, the value of the isosteric heat of adsorption (Q_{st}) can be found during correlation stage, as the equation includes the isosteric heat of adsorption as a fitting parameter. When calculating the isosteric heat of adsorption from modified D-A model, it was found as a function of surface coverage. The average $\mathbf{Q_{st}}$ estimated using modified D-A and Tóth models were 19.742 kJ mol^{-1} and 19.023 kJ mol^{-1}, respectively. The composite showed promising CO_2 adsorption capacity and thermal characteristics which leads to development of compact CO_2 based adsorption cooling systems.

Acknowledgments

This work was financially supported by International Institute for Carbon-Neutral Energy Research (WPI-I2CNER) of Kyushu University, Japan and Program of al-Farabi Kazakh National University for Graduated Student's Foreign Training, MES of the RK.

References

Amankwah, K.A.G., Schwarz, J.A., 1995. A modified approach for estimating pseudo vapor pressures in the application of the Dubinin–Astakhov equation. Carbon doi:10.1016/0008-6223(95)00079-S.

Askalany, A.A., Henninger, S.K., Ghazy, M., Saha, B.B., 2017. Effect of improving thermal conductivity of the adsorbent on performance of adsorption cooling system. Appl. Therm. Eng. 110, 695–702. doi:10.1016/j.applthermaleng.2016.08.075.

Azahar, F.H.M., Mitra, S., Yabushita, A., Harata, A., Saha, B.B., Thu, K., 2018. Improved model for the isosteric heat of adsorption and impacts on the performance of heat pump cycles. Appl. Therm. Eng. 143, 688–700. doi:10.1016/j.applthermaleng.2018.07.131.

Chahbani, M.H., Labidi, J., Paris, J., 2004. Modeling of adsorption heat pumps with heat regeneration. Appl. Therm. Eng. 24, 431–447. doi:10.1016/j.applthermaleng.2003.08.012.

El-Sharkawy, I.I., Pal, A., Miyazaki, T., Saha, B.B., Koyama, S., 2016. A study on consolidated composite adsorbents for cooling application. Appl. Therm. Eng. 98, 1214–1220. doi:10.1016/j.applthermaleng.2015.12.105.

Fan, W., Chakraborty, A., Kayal, S., 2016. Adsorption cooling cycles: insights into carbon dioxide adsorption on activated carbons. Energy, Elsevier Ltd. doi:10.1016/j.energy.2016.02.112.

Gwadera, M., Kupiec, K., 2011. Adsorption cooling as an effective method of waste heat utilization. Tech. Trans. 108, 61–70.

Himeno, S., Komatsu, T., Fujita, S., 2005. High-pressure adsorption equilibria of methane and carbon dioxide on several activated carbons. J. Chem. Eng. Data 50, 369–376. doi:10.1021/je049786x.

Jin, Z., Tian, B., Wang, L., Wang, R., 2013. Comparison on thermal conductivity and permeability of granular and consolidated activated carbon for refrigeration. Chin. J. Chem. Eng. 21, 676–682. doi:10.1016/S1004-9541(13)60525-X.

Jribi, S., Miyazaki, T., Saha, B.B., Pal, A., Younes, M.M., Koyama, S., Maalej, A., 2017. Equilibrium and kinetics of CO_2 adsorption onto activated carbon. Int. J. Heat Mass Transf. 108, 1941–1946. doi:10.1016/j.ijheatmasstransfer.2016.12.114.

Jribi, S., Saha, B.B., Koyama, S., Bentaher, H., 2014. Modeling and simulation of an activated carbon-CO_2 four bed based adsorption cooling system. Energy Convers. Manag. 78, 985–991. doi:10.1016/j.enconman.2013.06.061.

Kadam, Y.H., Yadav, D.H., Mohite, S.J., Panchal, P.P., Dongare, V.K., 2016. Design of Waste Heat Driven Vapour Adsorption Cooling System for Vehicle Air-Conditioning and Refrigeration 89–93.

Lemmini, F., Errougani, A., 2005. Building and experimentation of a solar powered adsorption refrigerator. Renew. Energy 30, 1989–2003. doi:10.1016/j.renene.2005.03.003.

Myers, A.L., Monson, P.A., 2014. Physical adsorption of gases: the case for absolute adsorption as the basis for thermodynamic analysis. Adsorption 20, 591–622. doi:10.1007/s10450-014-9604-1.

Pal, A., El-Sharkawy, I.I., Miyazaki, T., Saha, B.B., 2016a. Adsorption characteristics of consolidated adsorbents + ethanol pairs. In: Proceedings of the 8th Asian Conference on Refrigeration and Air-Conditioning, pp. 8–11.

Pal, A., El-Sharkawy, I.I., Saha, B.B., Habib, K., Miyazaki, T., Koyama, S., 2016b. Thermodynamic analysis of adsorption cooling cycle using consolidated composite adsorbents – ethanol pairs. ARPN J. Eng. Appl. Sci. 11, 12234–12238.

Pal, A., El-Sharkawy, I.I., Saha, B.B., Jribi, S., Miyazaki, T., Koyama, S., 2016c. Experimental investigation of CO_2 adsorption onto a carbon based consolidated composite adsorbent for adsorption cooling application. Appl. Therm. Eng. 109, 304–311. doi:10.1016/j.applthermaleng.2016.08.031.

Pal, A., Shahrom, M.S.R., Moniruzzaman, M., Wilfred, C.D., Mitra, S., Thu, K., Saha, B.B., 2017. Ionic liquid as a new binder for activated carbon based consolidated composite adsorbents. Chem. Eng. J. 326, 980–986. doi:10.1016/j.cej.2017.06.031.

Pal, A., Uddin, K., Thu, K., Saha, B.B., 2019. Activated carbon and graphene nanoplatelets based novel composite for performance enhancement of adsorption cooling cycle. Energy Convers. Manag. 180, 134–148. doi:10.1016/j.enconman.2018.10.092.

Rahman, K.A., Loh, W.S., Ng, K.C., 2013. Heat of adsorption and adsorbed phase specific heat capacity of methane/activated carbon system. Procedia Eng. 56, 118–125. doi:10.1016/j.proeng.2013.03.097.

Rezaei, F., Webley, P., 2010. Structured adsorbents in gas separation processes. Sep. Purif. Technol. 70, 243–256. doi:10.1016/j.seppur.2009.10.004.

Saha, B.B., Jribi, S., Koyama, S., El-sharkawy, I.I., 2011. Carbon dioxide adsorption isotherms on activated carbons. J. Chem. Eng. Data 56, 1974–1981. doi:10.1021/je100973t.

Sahoo, S., Ramgopal, M., 2016. Experimental studies on an indigenous coconut shell based activated carbon suitable for natural gas storage. Sādhanā 41, 459–468. doi:10.1007/s12046-016-0483-x.

Saxena, R., Singh, V.K., Kumar, E.A., 2014. Carbon dioxide capture and sequestration by adsorption on activated carbon. Energy Procedia 54, 320–329. doi:10.1016/j.egypro.2014.07.275.

Shen, C., Grande, C.A., Li, P., Yu, J., Rodrigues, A.E., 2010. Adsorption equilibria and kinetics of CO_2 and N_2 on activated carbon beads. Chem. Eng. J. 160, 398–407. doi:10.1016/j.cej.2009.12.005.

Shen, D., Bülow, M., Siperstein, F., Engelhard, M., Myers, A.L., 2000. Comparison of experimental techniques for measuring isosteric heat of adsorption. Adsorption 6, 275–286. doi:10.1023/A:1026551213604.

Singh, V.K., Kumar, E., A., 2016. Measurement and analysis of adsorption isotherms of CO_2 on activated carbon. Appl. Therm. Eng. 97, 77–86. doi:10.1016/j.applthermaleng.2015.10.052.

Singh, V.K., Kumar, E.A., 2017a. Measurement of CO_2 adsorption kinetics on activated carbons suitable for gas storage systems. Greenh. Gases Sci. Technol. 7, 182–201. doi:10.1002/ghg.1641.

Singh, V.K., Kumar, E.A., 2017b. Experimental investigation and thermodynamic analysis of CO_2 adsorption on activated carbons for cooling system. J. CO_2 Util. 17, 290–304. doi:10.1016/j.jcou.2016.12.004.

Singh, V.K., Kumar, E.A., 2017c. Thermodynamic analysis of single-stage and single-effect two-stage adsorption cooling cycles using indigenous coconut shell based activated carbon-CO_2 pair. Int. J. Refrig. 84, 238–252. doi:10.1016/j.ijrefrig.2017.08.007.

Singh, V.K., Kumar, E.A., 2015. Comparative studies on CO_2 adsorption kinetics by solid adsorbents. Energy Procedia 90, 316–325. doi:10.1016/j.egypro.2016.11.199.

Singh, V.K., Kumar, E.A., Saha, B.B., 2018. Adsorption isotherms, kinetics and thermodynamic simulation of CO2-CSAC pair for cooling application. Energy 160, 1158–1173. doi:10.1016/J.ENERGY.2018.07.063.

Srinivasan, K., Dutta, P., Ng, K.C., Saha, B.B., 2012. Calculation of heat of adsorption of gases and refrigerants on activated carbons from direct measurements fitted to the Dubinin–Astakhov equation. Adsorpt. Sci. Technol. 30, 549–565. doi:10.1260/0263-6174.30.7.549.

Srinivasan, K., Saha, B.B., Ng, K.C., Dutta, P., Prasad, M., 2011. A method for the calculation of the adsorbed phase volume and pseudo-saturation pressure from adsorption isotherm data on activated carbon. Phys. Chem. Chem. Phys. 13, 12559. doi:10.1039/c1cp20383e.

Tóth, J., 2002. Adsorption: Theory, Modeling, and Analysis. Marcel Dekker, Inc.

Wang, L.W., Tamainot-Telto, Z., Thorpe, R., Critoph, R.E., Metcalf, S.J., Wang, R.Z., 2011. Study of thermal conductivity, permeability, and adsorption performance of consolidated composite activated carbon adsorbent for refrigeration. Renew. Energy 36, 2062–2066. doi:10.1016/j.renene.2011.01.005.

Zakaria, Z., George, T., 2011. The performance of commercial activated carbon absorbent for adsorbed natural gas storage. Int. J. Res. Rev. Appl. Sci. 9, 225–230.

Zhou, L., Bai, S., Su, W., Yang, J., Zhou, Y., 2003. Comparative study of the excess versus absolute adsorption of CO_2 on superactivated carbon for the near-critical region. Langmuir 19, 2683–2690. doi:10.1021/la020682z.

Zhou, L., Zhou, Y., 1998. Linearization of adsorption isotherms for high-pressure applications. Chem. Eng. Sci. 53, 2531–2536. doi:10.1016/S0009-2509(98)00065-7.

Zhou, L., Zhou, Y., 1996. A Comprehensive Model for the Adsorption of Supercritical Hydrogen on Activated Carbon. Ind. Eng. Chem. Res. 35 (11), 4166–4168.